Available online at www.sciencedirect.com

ScienceDirect

Procedia Structural Integrity 2 (2016) 1853–1860

Structural Integrity Procedia

www.elsevier.com/locate/procedia

21st European Conference on Fracture, ECF21, 20-24 June 2016, Catania, Italy

Synthesis of crack initiation life in steel notched specimens under torsional fatigue based on the averaged strain energy density

Filippo Berto[a,b], Alberto Campagnolo[c], Giovanni Meneghetti[c]*, Keisuke Tanaka[d]

[a]*University of Padova, Department of Management and Engineering, Stradella S. Nicola 3, 36100, Vicenza (Italy)*
[b]*NTNU, Department of Engineering Design and Materials, Richard Birkelands vei 2b, 7491, Trondheim, (Norway)*
[c]*University of Padova, Department of Industrial Engineering, Via Venezia 1, 35131, Padova (Italy)*
[d]*Meijo University, Department of Mechanical Engineering, 468-8502, Nagoya (Japan)*

Abstract

The torsional fatigue behaviour of circumferentially notched specimens made of austenitic stainless steel, SUS316L, and carbon steel, SGV410, characterized by different notch root radii has been recently investigated by Tanaka. In that contribution, it was observed that the total fatigue life of the austenitic stainless steel increases with increasing stress concentration factor for a given applied nominal shear stress amplitude. By using the electrical potential drop method, Tanaka observed that the crack nucleation life was reduced with increasing stress concentration, on the other hand the crack propagation life increased. The experimental fatigue results, originally expressed in terms of nominal shear stress amplitude, have been reanalysed by means of the local strain energy density (SED) averaged over a control volume having radius R_0 surrounding the notch tip. To exclude all extrinsic effects acting during the fatigue crack propagation phase, such as sliding contact and/or friction between fracture surfaces, crack initiation life has been considered in the present work (*). In the original paper, initiation life was defined in correspondence of a 0.1÷0.4-mm-deep crack. The control radius R_0 for fatigue strength assessment of notched components, thought of as a material property, has been estimated by imposing the constancy of the averaged SED for both smooth and cracked specimens at $N_A = 2$ million loading cycles.

(*) A version of the present contribution has already been presented at the 11th International Conference on Multiaxial Fatigue and Fracture (ICMFF11).

Peer-review under responsibility of the Scientific Committee of ECF21.

* Corresponding author. Tel.: 0039 049 8276751
E-mail address: giovanni.meneghetti@unipd.it

Copyright © 2016 The Authors. Published by Elsevier B.V. This is an open access article under the CC BY-NC-ND license (http://creativecommons.org/licenses/by-nc-nd/4.0/).
Peer review under responsibility of the Scientific Committee of ECF21.
10.1016/j.prostr.2016.06.233

Keywords: Torsional fatigue; notch effect; crack initiation; averaged SED; electrical potential drop.

1. Introduction

Dealing with torsional and multiaxial fatigue, an anomalous phenomenon of the notch-strengthening effect was observed in circumferentially notched specimens made of austenitic stainless steels (Ohkawa and Ohkawa, 2011; Tanaka, 2010; Tanaka et al., 2009). The fatigue life of notched specimens resulted longer than that of smooth ones, and the longer the higher was the stress concentration factor under the same amplitude of the nominal shear stress. This notch-strengthening effect was also observed in NiCrMo steel (Berto et al., 2011), pure titanium (Okano and Hisamatsu, 2012), but it was not found in carbon steels (Atzori et al., 2006; Ohkawa and Ohkawa, 2011; Tanaka et al., 2011). In circumferentially notched bars subjected to torsion fatigue loadings, factory-roof type fracture surfaces are obtained under low stress amplitudes and the sliding contact of the fracture surfaces causes the retardation of crack propagation (Ritchie et al., 1982; Tanaka et al., 1996; Tschegg, 1983, 1982; Yu et al., 1998). At high stress amplitudes, instead, flat fracture surfaces are observed and the crack retardation due to sliding contact is reduced. The presence of a superimposed static tensile stress also reduces the crack surfaces contact (Tanaka et al., 1996).

Recently, Tanaka (2014) has deeply investigated this phenomenon dealing with the fatigue behaviour of notched bars made of austenitic stainless steel, SUS316L, and carbon steel, SGV410, subjected to torsion loadings and characterized by different notch tip radii. In the present work, the experimental fatigue results have been reanalysed by means of the averaged strain energy density (SED) approach, first proposed by Lazzarin and Zambardi (2001). The crack initiation life has been considered, in order to exclude all extrinsic effects acting during the fatigue crack propagation phase, such as sliding contact and/or friction between fracture surfaces.

2. Experimental fatigue results

The materials tested in (Tanaka, 2014) were an austenitic stainless steel (SUS316L) and a carbon steel (SGV410) for structural use in nuclear power plants. The yield strength and tensile strength of SUS316L were 260 and 591 MPa, and those of SGV410 were 275 and 470 MPa.

Figure 1 reports the geometry of the cylindrical specimens weakened by circumferential notches with three different root radii. The specimens with a notch radius ρ equal to 4.5, 1.07, and 0.22 mm are named NA, NB, and NC, respectively. The elastic stress net-section concentration factor for the shear stress under torsion for NA, NB, and NC specimens calculated by the finite element method (FEM) was 1.17, 1.55, and 2.54, respectively, while that for the tensile stress was 1.50, 2.50, and 5.07, respectively.

The experimental fatigue test results were obtained by adopting a nominal load ratio R equal to -1. The applied shear stress amplitude was expressed in terms of nominal stress calculated elastically from the applied torque for the minimum cross section. The fatigue tests under torsion loadings were conducted with and without superimposed static tension. In the first case, the applied static tensile stress (σ_m) equalled the applied shear stress amplitude (τ_a).

Tanaka (2014) employed a DC electrical potential method to monitor the fatigue crack initiation and propagation phases. The initiation life was defined in correspondence of a 0.1÷0.4-mm-deep crack. It was observed that the total fatigue life of the austenitic stainless steel (SUS316L) increases with increasing stress concentration factor for a given applied nominal shear stress amplitude. In particular, Tanaka (2014) observed that the crack nucleation life was reduced with increasing stress concentration; on the other hand the crack propagation life increased. The notch-strengthening effect has been attributed to the retarded propagation promoted by the crack surfaces contact, which occurs especially for the sharper notches. Indeed, the superposition of static tension on the fatigue torsion loading resulted in a notch-weakening behaviour, being the contact between the crack surfaces reduced. The notch strengthening effect was not observed in the SGV410 carbon steel.

On the basis of fracture surfaces and crack paths analyses (Tanaka, 2014), the difference in the notch effect on the fatigue behaviour of SUS316L and SGV410 appeared to be tied to different crack path morphologies of small cracks and three-dimensional fracture surface topographies observed by using scanning electron microscopy (SEM).

More details concerning both the experimental results, expressed in terms of nominal shear stress amplitude, and

the fracture surfaces analysis can be found in the original paper (Tanaka, 2014).

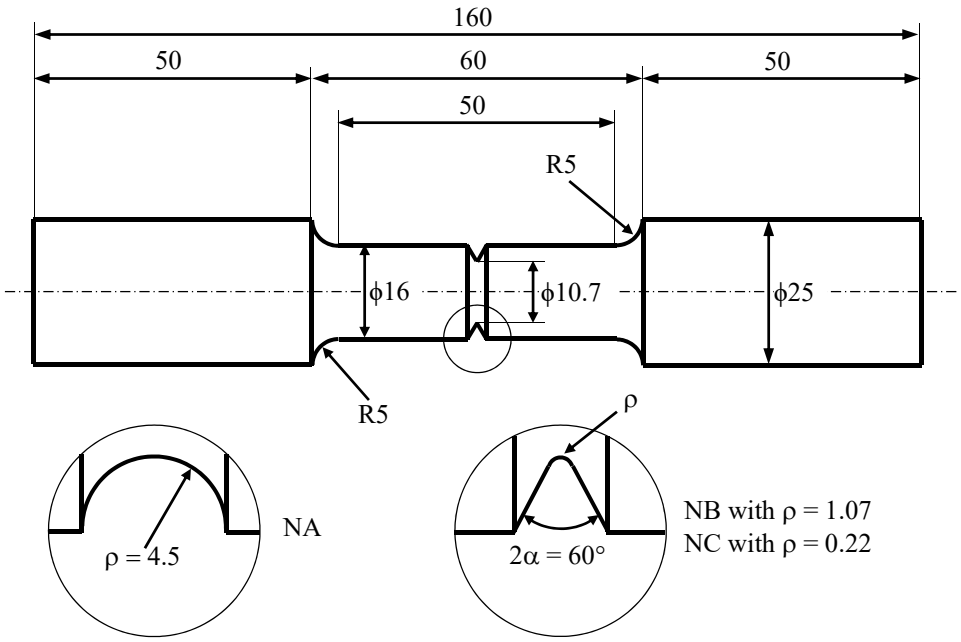

Fig. 1. Geometry of the cylindrical notched specimens (Tanaka, 2014) (dimensions are in mm).

3. Averaged strain energy density approach

The strain energy density (SED) averaged over a control volume, thought of as a material property according to Lazzarin and Zambardi (2001), proved to efficiently account for notch effects both in static (Berto and Lazzarin, 2014; Lazzarin and Zambardi, 2001) and fatigue (Atzori et al., 2006; Lazzarin and Zambardi, 2001) structural strength problems. The idea is reminiscent of the stress averaging to perform inside a material dependent structural volume, according to the approach proposed by Neuber.

Such a method was formalized and applied first to sharp, zero radius, V-notches (Lazzarin and Zambardi, 2001) and later extended to blunt U and V-notches (Lazzarin and Berto, 2005a). When dealing with sharp V-notches, the control volume is a circular sector of radius R_0 centered at the notch tip (Lazzarin and Zambardi, 2001). For a blunt V-notch, instead, the volume assumes the crescent shape shown in Fig. 2 (Lazzarin and Berto, 2005a), where R_0 is the depth measured along the notch bisector line. The outer radius of the crescent shape is equal to $R_0 + r_0$, where r_0 depends on the notch opening angle 2α and on the notch root radius ρ according to the following expression:

$$r_0 = \frac{q-1}{q}\rho \tag{1}$$

with q defined as:

$$q = \frac{2\pi - 2\alpha}{\pi} \tag{2}$$

The control radius R_0 for fatigue strength assessment of notched components has been defined by equalling the averaged SED in two situations, i.e. the fatigue limit of un-notched and cracked specimens, respectively (Berto et

al., 2011; Lazzarin and Berto, 2005b). Therefore R_0 combines two material properties: the plain material fatigue limit (or the high-cycle fatigue strength of smooth specimens) and the threshold value of the SIF range for long cracks. The following expressions have been derived under plain strain hypothesis (Berto et al., 2011; Lazzarin and Berto, 2005b) dealing with tension (mode I) and torsion (mode III) loadings, respectively:

$$R_{0,I} = 2e_1 \cdot \left(\frac{\Delta K_{I,th}}{\Delta \sigma_0} \right)^2 = \frac{(1+\nu)(5-8\nu)}{4\pi} \cdot \left(\frac{\Delta K_{I,th}}{\Delta \sigma_0} \right)^2 \tag{3}$$

$$R_{0,III} = \frac{e_3}{1+\nu} \cdot \left(\frac{\Delta K_{III,th}}{\Delta \tau_0} \right)^2 \tag{4}$$

It should be noted that, in principle, the control radius R_0 could assume different values under mode I and mode III, so that the energy contributions related to the two different loadings should be averaged in control volumes of different size (Berto et al., 2011). The idea of a control volume size dependent on the loading mode has been proposed for the first time in (Berto et al., 2011) dealing with the multiaxial fatigue strength assessment of notched specimens made of 39NiCrMo3 steel. It is important to underline that using a Poisson's coefficient $\nu = 0.30$, Eq. (3) (being valid under plain strain hypothesis) can be re-written as follows (Lazzarin and Berto, 2005b; Livieri and Lazzarin, 2005):

$$R_{0,I} = 0.85 \cdot \frac{1}{\pi} \cdot \left(\frac{\Delta K_{I,th}}{\Delta \sigma_0} \right)^2 \rightarrow = 0.85 \cdot a_0 \tag{5}$$

Therefore, R_0 in Fig. 2 results on the order of the El Haddad-Smith-Topper length parameter (El Haddad et al., 1979).

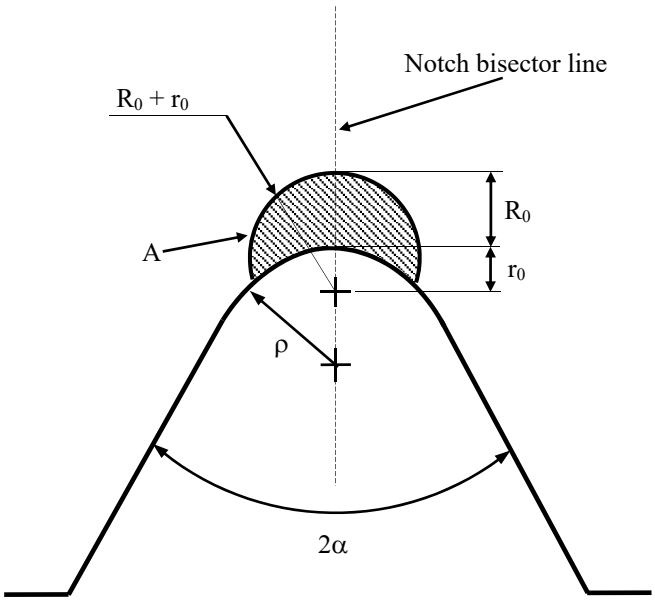

Fig. 2. Control volume for specimens weakened by rounded V-notches (Lazzarin and Berto, 2005a).

Once the control volume is properly defined, the averaged SED can be evaluated directly from the FE results,

$\Delta\overline{W}$, by summation of the strain-energies $W_{FEM,i}$ calculated for each i-th finite element belonging to the control area (A in Figs. 2 and 3):

$$\Delta\overline{W} = c_W \frac{\sum_A W_{FEM,i}}{A} \tag{6}$$

where the coefficient c_w accounts for the effect of the nominal load ratio R (Lazzarin et al., 2004), when the range value of the nominal stress is applied to the FE model. It is equal to 1 for R = 0 and to 0.5 for R = −1. Equation (6) defines the so-called direct approach to calculate the averaged SED. According to a recent contribution of Lazzarin et al. (2010), very coarse FE meshes can be adopted within the control volume A (see Fig. 3b).

4. SED-based synthesis of crack initiation experimental data

The fatigue properties of the considered materials have been taken from (Tanaka et al., 1999; Yu et al., 1998) and are reported in Table 1. All parameters are expressed in terms of range, defined as maximum minus minimum value. The control radii $R_{0,I}$ and $R_{0,III}$ have been calculated from Eqs. (3) and (4), respectively, where parameters e_1 and e_3 equal 0.133 and 0.414, respectively, for a Poisson's ratio $\nu = 0.3$.

Table 1. Mechanical properties

Material	$\Delta\sigma_0$ (MPa)	$\Delta K_{I,th}$ (MPa $m^{0.5}$)	$R_{0,I}$ (mm)	$\Delta\tau_0$ (MPa)	$\Delta K_{III,th}$ (MPa $m^{0.5}$)	$R_{0,III}$ (mm)
SUS 316L	442	10.30	0.144	266	9.86	0.438
SGV 410	436	10.60	0.157	270	12.80	0.716

The averaged SED values were calculated using the direct approach, $\Delta\overline{W}$, according to Eq. (6) (with about 500 finite elements inside the control volume). FE analyses have been carried out by means of Ansys® software and by adopting free mesh patterns consisting of two-dimensional, harmonic, 8-node linear quadrilateral elements (PLANE 83 of Ansys® element library), as shown in Fig. 3. The adopted finite element enables to analyse axis-symmetric components subjected to external loads that can be expressed according to a Fourier series expansion. Therefore, it can be employed for modelling three-dimensional axis-symmetric components under axial, bending or torsional loadings, keeping the advantage of treating two-dimensional FE analyses.

The results of the synthesis based on the local strain energy density are reported in Fig. 4. In order to exclude all extrinsic effects acting during the fatigue crack propagation phase, such as sliding contact and/or friction between fracture surfaces, crack initiation life, defined in correspondence of a crack depth in the range of 0.1÷0.4-mm as proposed by Tanaka (2014), has been considered in the present reanalysis. Moreover, it is important to underline that the range of the averaged strain energy density, $\Delta\overline{W}$, has been taken into account, so that the constant energy contribution of static tensile stresses has been neglected. This engineering approximation is acceptable if crack initiation life, and not the total life, is considered, because the static tensile stress contributes more to the crack growth behaviour (i.e. sliding contact and friction between the mating surfaces) than to the crack initiation phase. The control radius $R_{0,I}$ has been calculated and reported in Table 1 only for comparison purposes.

It can be observed that in the case of SUS 316L steel, the crack initiation experimental results are well summarized in a scatter-band (Fig. 4a), characterised by an equivalent stress-based scatter index T_σ ($= \sqrt{T_w}$) equal to 1.23; this value is practically coincident with the intrinsic scatter of the original data expressed in terms of nominal stresses, which was found equal to $T_\sigma = 1.24$. However, the effects of sliding contact and/or friction between fracture surfaces during the propagation phase are evident, because the experimental results in terms of total fatigue life (see the smaller symbols: the black ones are related to pure torsion fatigue loading, while the gray ones are for torsion fatigue loading with superimposed static tension) are characterized by a high scatter, due to the difference between the fatigue lives of specimens tested with and without static tensile stress.

In the case of SGV 410 steel (Fig. 4b) the crack initiation experimental data are more scattered, T_σ being higher and equal to 1.51,while the intrinsic scatter of the original data expressed in terms of nominal stress resulted equal to $T_\sigma = 1.17$. However, in this case, the influence of extrinsic effects is almost negligible and the experimental data in terms of total fatigue life fall within the scatter-band determined using crack initiation data.

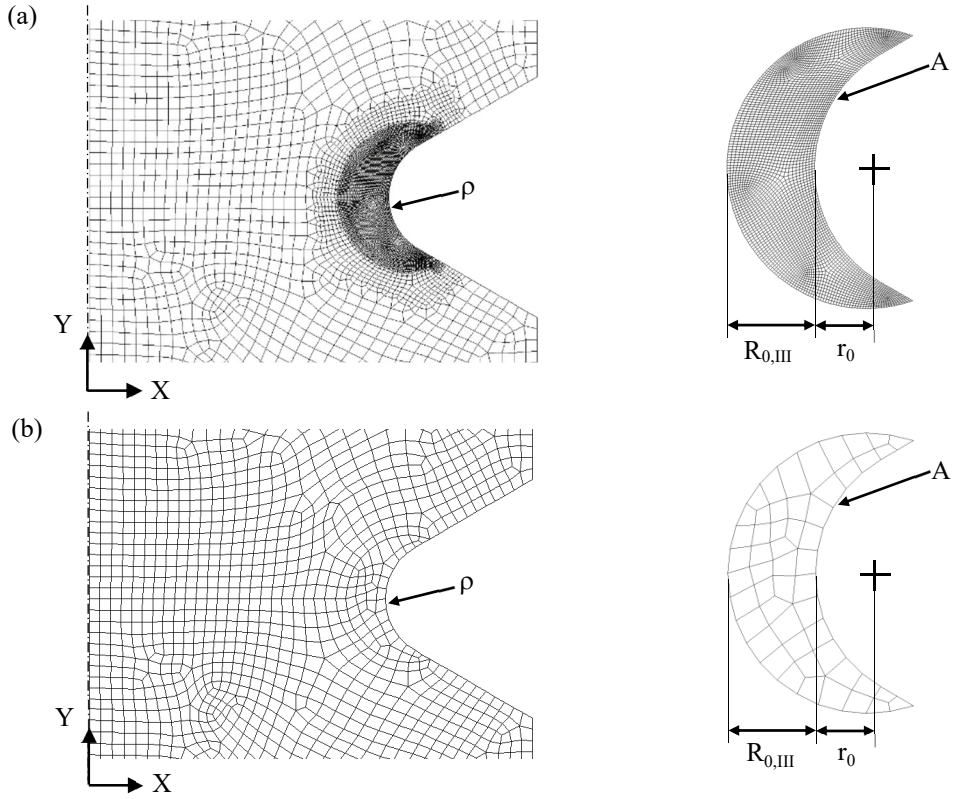

Fig. 3. FE mesh adopted in the numerical analyses: (a) refined one (about 500 FE inside the control volume) to evaluate the exact SED value and (b) coarse one (about 50 FE inside the control volume) producing a reduced error of 1%. The Y-axis coincides with the axis of the specimen. Considered case: NB specimen made of SGV 410 steel, with $\rho = 1.07$ mm, $R_{0,III} = 0.716$ mm, $r_0 = 0.428$ mm.

5. Conclusions

In the present contribution, some recent experimental fatigue test results, obtained from circumferentially notched specimens made of stainless and carbon steels, with different notch root radii and subjected to torsional fatigue loadings, have been reanalysed by means of the averaged strain energy density (SED) approach. Crack initiation life has been taken into account to exclude all extrinsic effects acting during the crack propagation phase, particularly of severely notched specimens made of stainless steel. The synthesis based on the local SED allowed to correlate fairly well the notch fatigue data for each tested material.

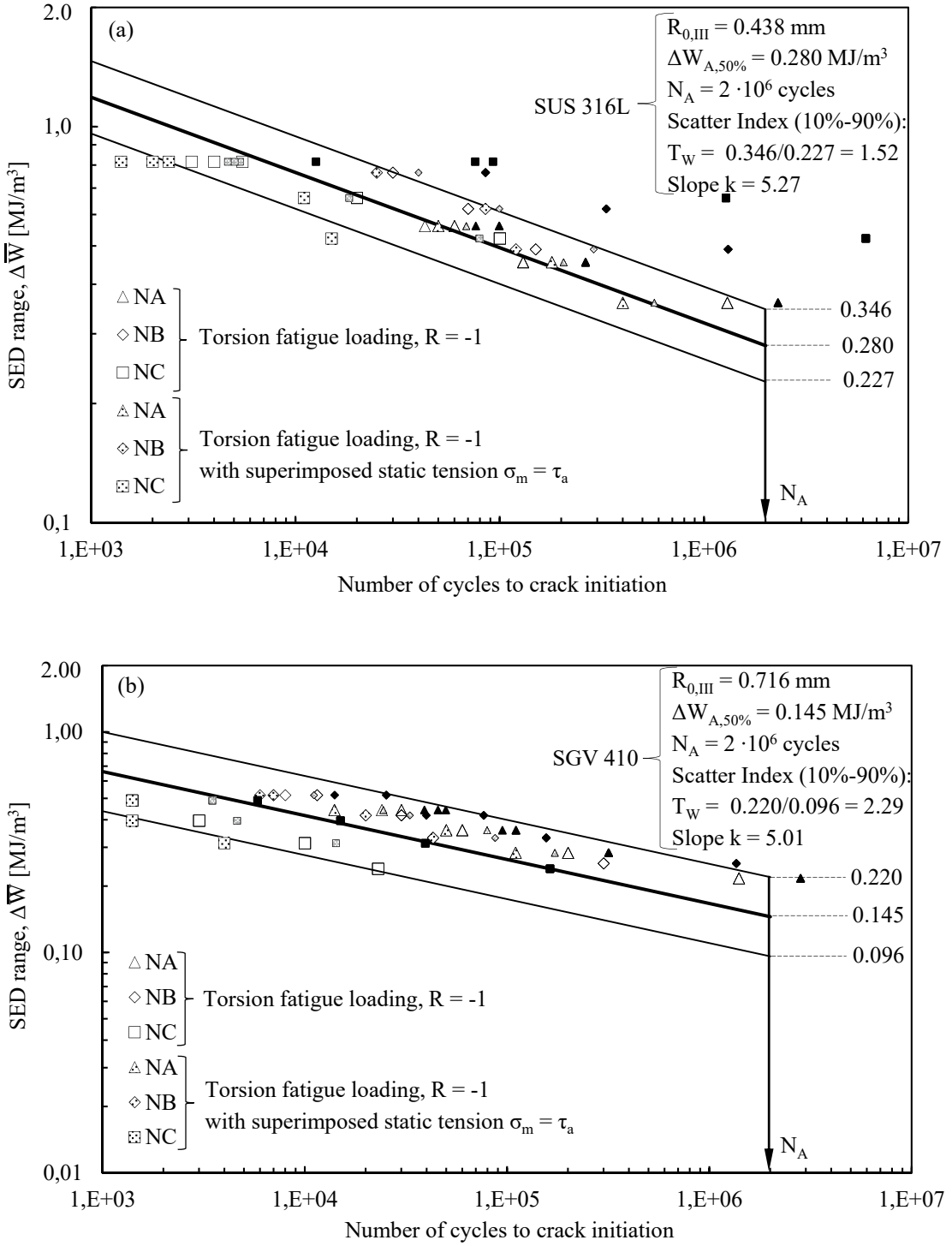

Fig. 4. Averaged SED-based scatter-band calibrated on the crack initiation experimental fatigue results for (a) SUS 316L and (b) SGV 410 steels. The smaller symbols indicate the total fatigue life for comparison purposes: the black ones are for pure torsion loading, while the gray ones are for torsion loading with superimposed static tension.

References

Atzori, B., Berto, F., Lazzarin, P., Quaresimin, M., 2006. Multi-axial fatigue behaviour of a severely notched carbon steel. Int. J. Fatigue 28, 485–493.

Berto, F., Lazzarin, P., 2014. Recent developments in brittle and quasi-brittle failure assessment of engineering materials by means of local approaches. Mater. Sci. Eng. R Reports 75, 1–48.

Berto, F., Lazzarin, P., Yates, J.R., 2011. Multiaxial fatigue of V-notched steel specimens: A non-conventional application of the local energy method. Fatigue Fract. Eng. Mater. Struct. 34, 921–943.

El Haddad, M.H., Topper, T.H., Smith, K.N., 1979. Prediction of non propagating cracks. Eng. Fract. Mech. 11, 573–584.

Lazzarin, P., Berto, F., 2005a. Some expressions for the strain energy in a finite volume surrounding the root of blunt V-notches. Int. J. Fract. 135, 161–185.

Lazzarin, P., Berto, F., 2005b. From Neuber's Elementary Volume to Kitagawa and Atzori's Diagrams: An Interpretation Based on Local Energy. Int. J. Fract. 135, L33–L38.

Lazzarin, P., Berto, F., Zappalorto, M., 2010. Rapid calculations of notch stress intensity factors based on averaged strain energy density from coarse meshes: Theoretical bases and applications. Int. J. Fatigue 32, 1559–1567.

Lazzarin, P., Sonsino, C.M., Zambardi, R., 2004. A notch stress intensity approach to assess the multiaxial fatigue strength of welded tube-to-flange joints subjected to combined loadings. Fatigue Fract. Eng. Mater. Struct. 27, 127–140.

Lazzarin, P., Zambardi, R., 2001. A finite-volume-energy based approach to predict the static and fatigue behavior of components with sharp V-shaped notches. Int. J. Fract. 112, 275–298.

Livieri, P., Lazzarin, P., 2005. Fatigue strength of steel and aluminium welded joints based on generalised stress intensity factors and local strain energy values. Int. J. Fract. 133, 247–276.

Ohkawa, C., Ohkawa, I., 2011. Notch effect on torsional fatigue of austenitic stainless steel: Comparison with low carbon steel. Eng. Fract. Mech. 78, 1577–1589.

Okano, T., Hisamatsu, N., 2012. Effect of notch of torsional fatigue property of pure titanium. Proc. 31 Symp. fatigue, Soc. Mater. Sci. Japan 31, 129–133.

Ritchie, R.O., McClintock, F.A., Nayeb-Hashemi, H., Ritter, M.A., 1982. Mode III fatigue crack propagation in low alloy steel. Metall. Trans. A 13, 101–110.

Tanaka, K., 2014. Crack initiation and propagation in torsional fatigue of circumferentially notched steel bars. Int. J. Fatigue 58, 114–125.

Tanaka, K., 2010. Small fatigue crack propagation in notched components under combined torsional and axial loading. Procedia Eng. 2, 27–46.

Tanaka, K., Akiniwa, Y., Nakamura, H., 1996. J-integral approach to mode III fatigue crack propagation in steel under torsional loading. Fatigue Fract. Eng. Mater. Struct. 19, 571–579.

Tanaka, K., Akiniwa, Y., Yu, H., 1999. The propagation of a circumferential fatigue crack in medium-carbon steel bars under combined torsional and axial loadings. In: Mixed-Mode Crack Behaviou, in: Miller, K., McDowell, D. (Eds.), Mixed-Mode Crack Behaviour, ASTM 1359. West Conshohocked, PA, pp. 295–311.

Tanaka, K., Hashimoto, A., Narita, J., Egami, N., 2009. Fatigue life of circumferentially notched bars of austenitic stainless steel under cyclic torsion with and without static tension. J Soc Mater Sci 58, 1044–1050.

Tanaka, K., Ishikawa, T., Narita, J., Egami, N., 2011. Fatigue life of circumferentially notched bars of carbon steel under cyclic torsion with and without static tension. J Soc Mater Sci 60.

Tschegg, E.K., 1983. The influence of the static I load mode and R ratio on mode III fatigue crack growth behaviour in mild steel. Mater. Sci. Eng. 59, 127–137.

Tschegg, E.K., 1982. A contribution to mode III fatigue crack propagation. Mater. Sci. Eng. 54, 127–136.

Yu, H., Tanaka, K., Akiniwa, Y., 1998. Estimation of torsional fatigue strength of medium carbon steel bars with a circumferential crack by the cyclic resistance-curve method. Fatigue Fract. Eng. Mater. Struct. 21, 1067–1076.